

# Cone Beam Computed Tomographic Analysis of Anatomical Variations of Greater Palatine Canal and Foramen in Relation to Gender in South Indian Population

ML Asha, G Arun Kumar, V Sattigeri Anupama, V Raja Jigna, Malhotra Diksha

Department of Oral Medicine and Radiology, Dr. Syamala Reddy dental college hospital and research center, Bangalore, India

## Abstract

**Aim:** The greater palatine canal (GPC) contains the greater and lesser palatine nerves, which enters the hard palate at respective greater palatine foramina (GPF). The anatomical variations of GPC and foramina have not been studied comprehensively in South-Indian population. A study was done to evaluate the GPF and canals in South Indian patients using cone beam computed tomography (CBCT) providing their variations in relation to gender.

**Methods:** This experimental study included 100 CBCT scans of maxilla (50 males and 50 females) from patients who had informed consent for this study. Inclusion criteria include age above 18 years old, exclusion criteria were: history of trauma or orthognathic surgery, pathologies and CBCT scans that didn't include maxilla. The selected scans had paraxial slices of slice thickness 0.3 mm. The greater palatine region was examined in CBCT scans using Carestream 93003D imaging system, 70-90 kVp, 5-10 mA, voxel size 90-180  $\mu$ m, field of view 10 $\times$ 5 cm. The effect of anatomical variations of greater palatine region on patient's gender were evaluated using 7 different parameters.

**Results:** The present study shows that in South-Indian patients, the GPF was more closely related to the second molar. Therefore, the second molar can serve as landmark for successful GPF anesthesia. The measurement GPF to alveolar ridge (AR) was significant among genders. The mean canal length was significantly significant according to sex and side. Therefore GPF location, AR distance and canal length could be used as reliable clinical index.

**Conclusion:** This study proves that 3D images of CBCT can detect precise anatomic routes to prevent the complications of procedures carried out in greater palatine region.

*Key Words:* Alveolar ridge (AR), Cone beam computed tomography, Greater palatine canal (GPC), Mid-maxillary suture (MMS), Pterygopalatine fossa (PPF)

## Introduction

The greater palatine canal (GPC) extends through the pterygopalatine fossa (PPF), which then diverges to enter the hard palate at respective foramina. It houses the descending palatine artery (a branch of the third division of the maxillary artery) and greater and lesser palatine nerves (branches of the maxillary division of the trigeminal nerve) and their posterior inferio-lateral nasal branches [1]. The canal helps direct access to the PPF, including the sphenopalatine ganglion, pterygopalatine ganglion, infraorbital nerve, internal maxillary artery, and the pterygoid venous plexus [1]. The anatomy of the GPC is of interest to dentists, oral maxillofacial surgeons, and otolaryngologists performing procedures in this area (e.g., administration of local anesthesia, dental implant placement, orthognathic Le Fort osteotomies, and sino-nasal surgeries) [2].

Clinical textbooks on anesthesia locates the GPF in relation to the molar teeth [3]. However, in a comparison one finds variation in the reported locations. Accordingly the position is cited as opposite the second molar, opposite the third molar or anywhere between the second and third molar [4].

Variations in the location of GPF may pose difficulties in the local and regional anesthesia of the trigeminal maxillary division. In addition, difficulties may occur in identifying the emergence of the greater palatine artery within the oral cavity, which represents important information in the surgery of

palatal free vascular flaps, cleft palate, or maxillary sinus [5].

A good knowledge of the anatomy and average length of the GPC is crucial in order to avoid possible complications such as penetration of the orbit and nasal cavity, proptosis, blindness from vasoconstriction of the ophthalmic artery and/or intracranial spread of infection, intravascular injection, penetration of the nasopharynx, damage to neural tissue, and failed anesthesia. 3D images of cone beam computed tomography (CBCT) are becoming more readily available for use in maxillofacial applications and provides better image quality of teeth and their surrounding structures, compared with conventional CT scan [1].

## Aims

The aim of this study was to map the anatomical variations of the greater palatine canal and greater palatine foramen using CBCT in the South-Indian population. Our results have been compared to the already existing anatomical data in other races and populations, might improve clinical success in maxillofacial and oral surgery.

## Materials and Methods

A descriptive analytical cross-sectional study was conducted on 100 CBCT scans of maxilla (50 males and 50 females). The patients who visited a diagnostic centre were randomly

Corresponding author: Arun Kumar G, Department of Oral Medicine and Radiology, Dr. Syamala Reddy dental college hospital and research center, No111/1, S.G.R College main road, Marathalli post, Bangalore-560037, Karnataka, India, Tel: +91-88892830433; e-mail: arunkumarg11061987@gmail.com

selected after considering the following criteria. The inclusion criteria included: presence of all upper erupted molars in both maxilla sides; male/female aged 18 years or older, and absence of any pathological conditions or deformities in the jaws. The exclusion criteria were: history of trauma or orthognathic surgery, presence of pathologic bone disease in maxilla, CBCT scans that did not include maxilla and syndromic patients. All patients had their CBCT scans taken for other purposes and they had informed consent for participation in this study. The selected scans had paraxial slices with slice thickness of 0.3 mm. The greater palatine region was in the CBCT scans. The CBCT examinations were carried out for every patient with Carestream 9300 3D imaging system. Full rotation scan was performed with 70-90 kVp, 5-10 mA and voxel size of 90-180 m. the size of field of view will be 10x5 cm. All images were taken using volume 1 (high-resolution) and high-contrast options.

To standardize the shape of the GPF, two different landmarks were introduced as its inferior limit; in the sagittal plane, the posterior wall of the GPF was used, and in the coronal plane, the inferior surface of the horizontal hard palate was used according to the method given by Sheiki et al. [1] Also for this study, the pterygoid canal was selected as the superior limit instead of the foramen rotundum due to its ease of identification in relation to the greater palatine canal. Soft tissue depth was not included [2].

Seven different variables were assessed, which are discussed subsequently.

**Position of GPF in relation to upper molars:** To assess the position of the GPF with respect to the upper molars, the following evaluation was conducted on each image in axial reconstruction. Firstly, five tangents were drawn parallel to the middle of and interproximal to the face of the upper molars and the following classification was used to assess the position (*Figure 1*): (A) From the medial face of second molar to its center; (B) From the center of second molar up to its distal face; (C) From the medial face of third molar up to its center; (D) From the center of third molar up to its distal face and (E) Distal from the third molar.

**Diameter of GPF:** The average diameter of the GPF was determined using axial reconstruction (*Figure 2*).

**Distance from GPF to MMS:** The study of anatomical landmarks such as the AR and the MMS is important because they can be used as a reference points to locate GPF in edentulous patients. Distance to AR and to MMS could be used to assess the location of GPF before anesthesia block or incision to harvest palatal soft tissue graft. Axial sections were created to evaluate the distance from the GPF to the MMS. In the axial reconstruction, a perpendicular line was drawn from the center of the GPF to the MMS (*Figure 3*). The resulting distance from each reconstruction was calculated.

**Distance from AR to GPF:** Distance from the GPF to the AR was measured in the axial reconstruction. In the depth of the upper molars, a line was drawn tangential to the AR. Following this, a perpendicular line was drawn in the depth of the GPF and the distance was determined from the AR to the medial GPF wall (*Figure 4*).

**The mean CL of GPC:** The method described by Haward-Swirzinski, et al. [6] was used to assess the CL and its paths

in sagittal plane. The length of the GPC was measured from the center of the pterygoid canal, as the center point of the PPF to the GPF on the inferior surface of the hard palate. It was measured in millimeters using the straightest linear path passing through the center of the canal (*Figure 5*).

The pathways of GPC in the coronal plane.

The pathways of GPC in the sagittal plane



*Figure 1. Position of GPF in relation to upper molars.*



*Figure 2. Diameter of GPF.*



*Figure 3. Distance from GPF to MMS.*

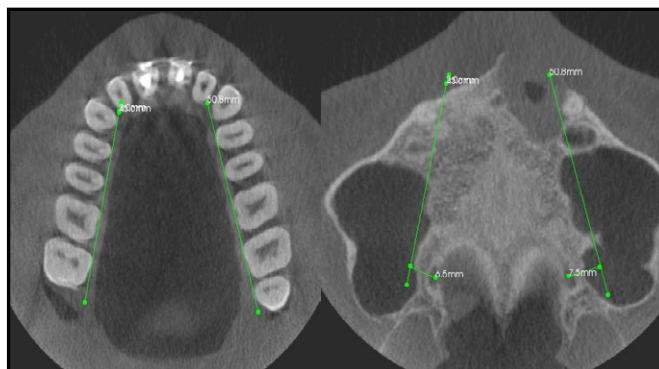


Figure 4. Distance from AR to GPF.

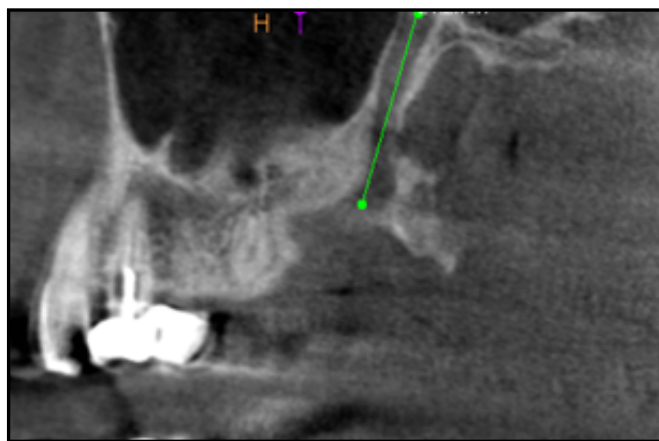


Figure 5. The CL of GPC.

### Statistical Analysis

The analysis was conducted using the distance measuring tool of CS 3D software and the images were saved as JPEG. The measurements were repeated 2 months later and intra-examiner agreement was performed (Dahlberg's error and paired T test). All data were evaluated using SPSS software version 19 package.

A paired T test ( $P < 0.05$ ) was conducted to compare the measurements from the right and left side, and a T test was conducted to compare the values between the sexes. Independent t-test was used to compare the CL values and the distance from GPF to MMS and AR. One-way analysis of variance (ANOVA) was used to compare the CL and IOF between the two study groups. To identify the level of agreement between the CL on the right and left sides, an intra-class correlation coefficient (ICC) was used. A kappa coefficient was used to identify the degree of symmetry between the pathways on the right and left sides as viewed in the sagittal and coronal planes. A kappa values were considered as follows  $< 0.20$  poor,  $0.21-0.40$  fair,  $0.41-0.60$  moderate,  $0.61-0.80$  good and  $0.81-1.00$  very good. A P-value less than the 0.05 level of significance was considered statistically significant. Further Discriminant analysis (ROC analysis) was used to assess the validity of linear measurements used in this study in differentiation of male gender from female according to method given by Sorlie(1995) [7].

### Results

#### Position of GPF in relation to upper molars

One hundred patients (50 males/50 females) with mean age of  $35.80 (\pm 10.99)$  years were examined. In 34% of the total

examinations, GPF was found to be located between the middle of the second molar and its distal surface (position B), 25% medial face of the third molar and its center (position C); 18% between the middle of the third molar and its distal surface (position D); 16% between the medial surface of the second molar to its center; 7% distal to the third molar. From the 200 GPFs examined, 68 were in the positions B and of those 36 were in the right side and 29 in the left side. The mean diameter of GPF on right side was found to be  $2.03 \text{ mm} (\pm 0.63)$ , and on left side was found to be  $1.94 \text{ mm} (\pm 0.61)$ . The mean distances from GPF to MMS were  $19.89 \text{ mm} (\pm 3.02)$  on right side and  $19.39 \text{ mm} (\pm 2.97)$  on the left side. The mean distance from GPF to AR were observed to be  $29.47 \text{ mm} (\pm 4.43)$  and  $28.65 \text{ mm} (\pm 4.5)$  in right and left sides respectively.

The measurement GPF to AR was found to be statistically significant among males and females ( $P=0.048$ ). The mean CL of the GPC was  $28.61 \pm 3.51 \text{ mm}$  ( $26.7 \pm 2.34 \text{ mm}$  on the right side and  $27.52 \pm 2.40 \text{ mm}$  on the left, intra-examiner reliability was 95%); a statistically significant difference in CL was observed between the right and left sides ( $P=0.044$ ). However, the ICC was 0.8422 with  $P < 0.001$ , which indicates a consistent mean CL.

The mean CL in females was  $26.55 \pm 1.74 \text{ mm}$  and in males was  $27.94 \pm 2.17 \text{ mm}$ , which was not a statistically significant difference ( $P=0.001$ ) (Table 1).

#### Incidence of pathways of GPC

Investigations of the canal path revealed four path types in the sagittal plane and five path types in the coronal plane.

Incidence of pathways of GPC observed in sagittal plane (Table 2).

Degree of symmetry between the pathways on right and left sides: The different pathways and the degree of symmetry between the pathways on the right and left sides in the sagittal and coronal planes are shown in Figures 3 and 4 and in Table 3 (kappa), respectively (Table 4).

#### Receiver operating characteristic curve (ROC Curve):

Discriminant analysis (ROC analysis) was used to assess the validity of linear measurements used in this study. The ROC curve gives a typical cut-off for differentiating male from female by giving a typical cutoff values would be 100% specific to establish the diagnosis of gender (Figure 15).

The typical cut-off value could predict the gender type with great accuracy, testing positive when it would predict gender with a value of high specificity and less sensitivity, testing negative when values would exclude gender with less specificity and high sensitivity (Table 5).

### Discussion

Since the greater palatine nerve block is associated with several complications, this study was performed to determine the mean dimensions of the GPC, its foramina and the geometric pattern of this structure, as well as to identify a reliable clinical index that can be used to estimate the mean values for each sex using CBCT data [1].

From our study using a subset of South-Indian population, we were able to assess the location of the GPF in relation to the face of each upper erupted molar. The GPF was found to be located in the palatal side of second molar in the 59/100 of the cases studied; most of them (34/100) were in position

B and 25/100 in position C. In our study, 16/100 of the GPF were medial to the second molar and 7/100 were distal to the third molar. In previous studies using Nigerian and Indian dry skulls [8,9] it was found that GPF was medial to the third molar in 48 and 64% of the cases, respectively. Also, 16%

GPFs were found to be medial to the second molar in our study, compared to 13.3% in the Nigerian study [8]. In a study using dry skulls, it was found that 5.6% were opposite to the second molar, 23.1% between the second to third molars and 64.4% opposite to the third molar. The percentage of GPFs

**Table 1.** The mean CL and its significance among genders.

Gender	n	Right	Left	P value	ICC
Male	50	28.46 ± 3.37	28.39 ± 1.37	0.117	0.407
Female	50	24.94 ± 2.12	25.86 ± 2.27	0.028	0.682

**Table 2.** Incidence of pathways of GPC observed in sagittal plane.

Figure	Pathway	Right Canal	Left Canal	Bilaterally Symmetrical	Overall Incidence
Figure 6	GPC travels in an anterior-inferior direction from the PPF	16	15	12	15.5%
Figure 7	GPC first travels in an inferior direction and then in an anterior-inferior direction through the remainder of the canal	28	34	16	31%
Figure 8	The GPC first travels in an inferior direction and then changes to an anterior-inferior direction and subsequently in inferior direction through the remainder of the canal	32	31	22	31.5%
Figure 9	The GPC travels in a directly inferior direction from the PPF	24	20	14	22%



**Figure 6.** GPC travels in an anterior-inferior direction from the PPF.

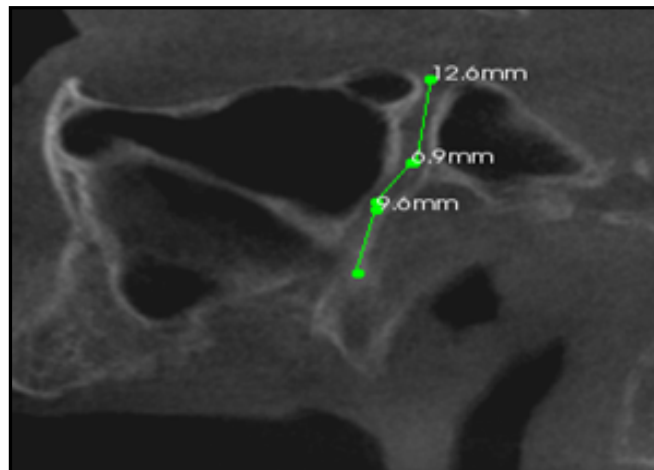


**Figure 8.** The GPC first travels in an inferior direction and then changes to an anterior-inferior direction and subsequently in inferior direction through the remainder of the canal.

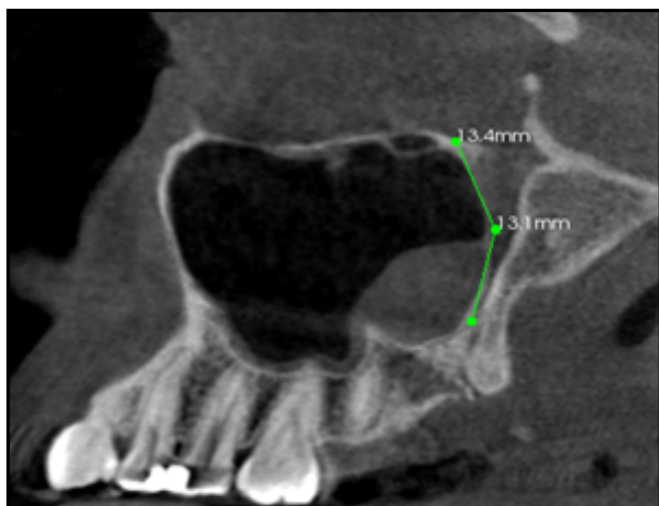


**Figure 7.** GPC first travels in an inferior direction and then in an anterior-inferior direction through the remainder of the canal.



**Figure 9.** The GPC travels in a directly inferior direction from the PPF.

**Table 3.** Incidence of pathways of GPC observed in the coronal plane

FIGURE	Pathway	Right Canal	Left Canal	Bilaterally Symmetrical	Overall Incidence
Figure 10	The GPC travels in an inferior-lateral direction from the PPF and then in a directly inferior direction	15	9	5	12%
Figure 11	The GPC travels in an inferior-lateral direction for a certain distance and then changes to an inferior-medial direction through the remainder of the canal	35	30	19	32.5%
Figure 12	The GPC first travels in an inferior-lateral direction and then in a directly inferior direction, and finally in an inferior-medial direction	23	34	15	26.5%
Figure 13	The GPC travels in a directly inferior direction from the PPF	16	15	8	15.5%
Figure 14	The GPC first travels in an inferior direction and then changes to an postero-inferior direction, and subsequently to an inferior direction through remainder of the canal	11	12	4	11.5%



**Figure 10.** The GPC travels in an inferior-lateral direction from the PPF and then in a directly inferior direction.

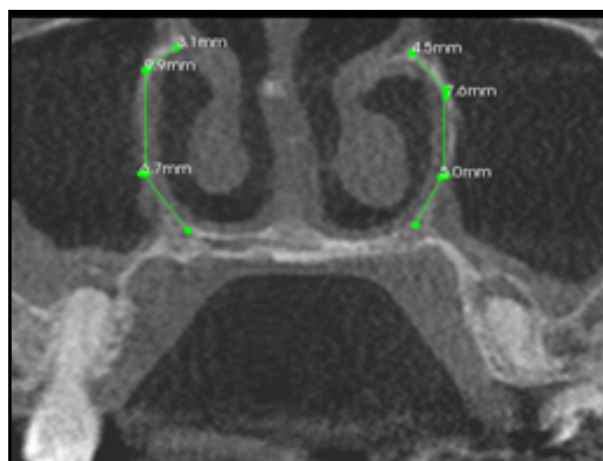


**Figure 12.** The GPC first travels in an inferior-lateral direction and then in a directly inferior direction, and finally in an inferior-medial direction.

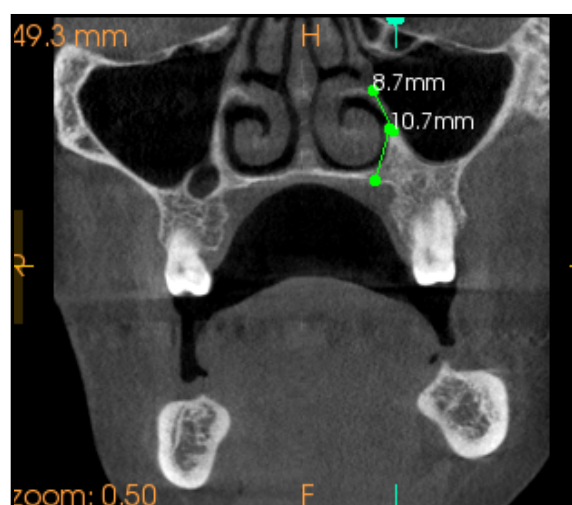


**Figure 11.** The GPC travels in an inferior-lateral direction for a certain distance and then changes to an inferior-medial direction through the remainder of the canal.



**Figure 13.** The GPC travels in a directly inferior direction from the PPF.

found distal to the third molar in our study (7%) is comparable to those mentioned in other studies 6.9% [9] and 2.9% [8]. The average diameter of the GPF was found to be 1.98 mm, which was comparable to previous studies [10,11].

Previous studies have showed the distances from the GPF to the MMS in Nigerian, Thai and Brazilian dry skulls to be 15.4, 14.7, and 14.68 mm, respectively [8,9,12]. These values are higher in South-Indian population (19.89 mm).

Considering the AR as a reference landmark, we found the distance from the AR to the GPF to be 29.47 mm. We

could not compare our AR to GPF distance to other studies [8,9,13] because usually they evaluate the distance from GPF to the posterior border of the palate instead of the distance from GPF to AR as we did.

Methathrathip et al. [14] studied 105 dried skulls and

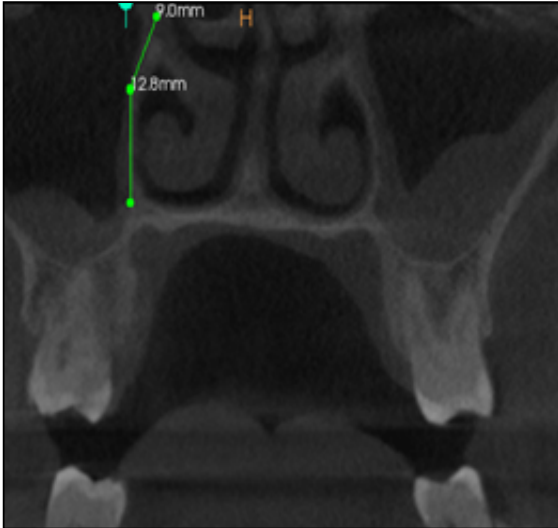


**Figure 14.** The GPC first travels in an inferior direction and then changes to anposterior-inferior direction, and subsequently to an inferior direction through remainder of the canal.

**Table 4.** Degree of symmetry between the pathways on right and left sides.

Plane	Sex	n	Kappa value	Strength of Agreement
Sagittal	Male	50	0.000	Poor
	Female	50	0.804	Good
	Total	100	0.007	Poor
Coronal	Male	50	0.989	Very good
	Female	50	0.025	Fair
	Total	100	0.112	Poor

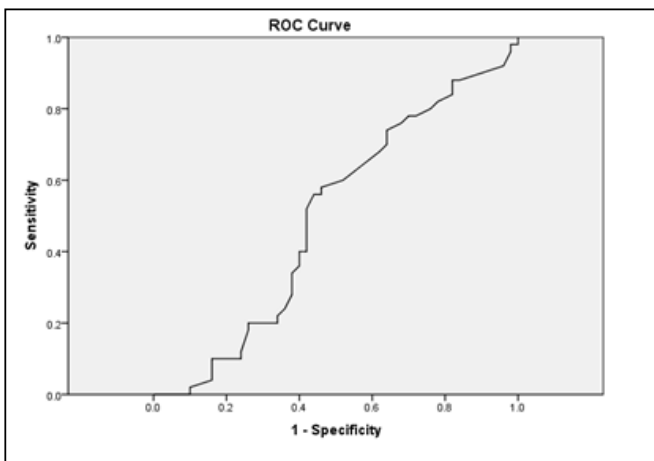


**Figure 15.** Receiver operating characteristic curve (ROC curve)

**Table 5.** Validity parameters to predict male and female genders using ROC analysis.

Parameter	Gender (male)	Gender (Female)	Typical Cut-off	Area Under the Curve (AUC)	P value
GPF to MMS (Right canal)	20.80 mm	18.55 mm	19.40 mm	0.495	0.929
GPF to MMS (Left canal)	19.30 mm	18.30 mm	17.60 mm	0.512	0.833
GPF to AR(Right canal)	31.10 mm	27.65 mm	28.70 mm	0.578	0.181
GPF to AR(Left canal)	29.85 mm	27.10 mm	28.10 mm	0.632	0.023

reported that the length of the GPC and PPF from the GPF to the inferior border of the foramen rotundum ranged from 16.3 to 40.9 mm, with a mean of  $29.7 \pm 4.2$  mm, which is consistent with the present study results (mean CL= $28.61 \pm 3.51$  mm). McKinney et al.analyzed the length of the GPC using high-resolution CT, and reported that the mean distance from the GPF to the sphenopalatine foramen to be 28.75 mm. Hwang, et al. repeated the study using 3D CT scans and reported a mean height of the PPF and mean CL that were also in agreement with our findings.

However, the mean CL reported by Douglas, et al. [7] (40.1 mm) were not consistent with the present study; these differences could be explained by the small number of subjects included in the study or by differences in ethnicity.

In our study, the mean CL was higher in males than in females. Previous studies [1] on sexual dimorphism have suggested that the craniofacial complex is highly variable in both size and shape by sex, and the zygomatic curve and skull size are generally larger in males than in females. Differences in the shape of the midsagittal curve, the skull roof, the upper one-third of the face, the nose, eyes, and palate are all statistically significantly different between males and females.

In the coronal plane, the most common pathway observed was consistent with that reported by Haward-Swirzinski et al. [3] but this was not in agreement with the pathway they observed in the sagittal plane, which could be explained by the small number of subjects included in our study or by the differences due to ethnicity or sex. Also in our study we have calculated typical cut-off values which helps in predicting male and female genders, the values of which could be helpful in medico-legal cases and mass disorders (forensic identification).

A limiting factor in the present study was the small sample size and we suggest that further studies to be performed on a larger group of subjects of different age and ethnicity. It is also suggested that GPF should be compared in adults and children as well as in subjects with specific craniofacial diseases.

### Conclusion

It is important to consider CBCT as an important diagnostic tool especially to study the most inaccessible areas which cannot be studied by other imaging modalities. The GPF may be an anatomical obstacle in oral and maxillofacial surgery procedures in the posterior area of the palate, but using CBCT the variations in its position can help the clinicians in providing improved surgical procedures and may also be helpful in forensic identification. The present study shows that in South-Indian patients, the GPF was more closely related to the second molar. Hence the GPF location, AR distance and canal length could be used as reliable clinical index.

## Acknowledgements

My sincere thanks and gratitude to Dr. Asha M.L, Head of department, Department of oral medicine and radiology for

her constant support and encouragement throughout my post-graduate course. A special thanks to Dr Jigna V. Raja, Dr Anupama VS and Dr. Diksha Malhotra for their support.

## References

1. Mahnaz Sheikhi, Asieh Zamaninaser, Faranak Jalalian. Length and anatomic routes of the greater palatine canal as observed by cone beam computed tomography. *Dental research journal*. 2013; **18**: 155-161.
2. Haward-Swirzinski K, Edwards PC, Saini TS, Norton NS. Length and geometric patterns of the greater palatine canal observed in cone beam computed tomography. *International Journal of Dentistry*. 2010.
3. Malamed FS. Textbook of local anesthesia. 4th ed. Rio de Janeiro: 2001; 164-167.
4. An analysis of the position of the greater palatine foramen Akram et al J.Basic.med. Sc 2003; **3**(1).
5. Nimigean V, Nimigean VR, Buțincu L, Sălăvăstru DI, Podoleanu L. Anatomical and clinical considerations regarding the greater palatine foramen. *Romanian journal of morphology and embryology*. 2013; **54** (3 Suppl): 779-783.
6. Carla Renata Sanomiya Ikuta, Camila Lopes Cardoso, Osny Ferreira-Júnior, José Roberto Pereira Lauris, Paulo Henrique Couto Souza, Izabel Regina Fischer Rubira-Bullen. Position of the greater palatine foramen: an anatomical study through cone beam computed tomography images. *Surgical and Radiologic Anatomy*. 2013; **35**: 837-842.
7. Douglas R, Wormald PJ. Pterygopalatine fossa infiltration through the greater palatine foramen: where to bend the needle. *Laryngoscope*. 2006; **116**: 1255-7.
8. Ajmani ML. Anatomical variation in position of the greater palatine foramen in the adult human skull. *Journal of Anatomy*. 1994; **184**: 635-637.
9. Saralaya V, Nayak SR. The relative position of the greater palatine foramen in dry Indian skulls. *Singapore Medical Journal*. 2007; **48**: 1143-1146.
10. Kim HS, Kim DI, Chung IH. High-resolution CT of the pterygopalatine fossa and its communications. *Neuroradiology*. 1996; **38**: 120-126.
11. Mendel N, Puterbaugh PG. Conduction, infiltration and general anesthesia in dentistry, 4th ed. Dental Items of Interest Publishing Co, New York, 1938; 140.
12. Klosek SK, Rungruang T. Anatomical study of the greater palatine artery and related structures of the palatal vault: considerations for palate as the subepithelial connective tissue graft donor site. *Surgical and Radiologic Anatomy*. 2009; **31**: 245-250.
13. Sharma NA, Garud RS. Greater palatine foramen-key to dimensions at the palatal vault as a donor site. *J Periodontol* successful hemimaxillary anaesthesia: a morphometric study and 77: 899-902 report of a rare aberration. *Singapore Medical Journal*. 2013; **54**: 152-159.
14. Methathrathip D, Apinhasmit W, Chompoopong S, Lertsirithong A, Ariyawatkul T, Sangvichien S. Anatomy of greater palatine foramen and canal and pterygopalatine fossa in Thais: considerations for maxillary nerve block. *Surgical and Radiologic Anatomy*. 2005; **27**: 511-516.